

Rare-earth chalcogenides: A large family of triangular lattice spin liquid candidates

Weiwei Liu,^{1,2†} Zheng Zhang,^{1,2†} Jianting Ji,^{1†} Yixuan Liu,² Jianshu Li,^{1,2} Hechang Lei,² Qingming Zhang^{1,3‡}

¹National Laboratory for Condensed Matter Physics and Institute of Physics, Chinese Academy of Sciences, Beijing 100190, China

²Department of Physics, Renmin University of China, Beijing 100872, China

³School of Physical Science and Technology, Lanzhou University, Lanzhou 730000, China

Abstract

Quantum spin-frustrated materials are expected to host many exotic quantum spin states like quantum spin liquid (QSL), and have attracted numerous interest in condensed matter physics. The discovery of YbMgGaO_4 invokes increasing attention on rare-earth-based spin frustrated materials with strong spin-orbit coupling. Here we report the discovery of a large family of quantum spin liquid candidates. We have systematically synthesized rare-earth chalcogenides AReCh_2 (A =alkali or monovalent ions, Re =rare earth, $\text{Ch}=\text{O, S, Se}$), and made structural and thermodynamics characterizations. The family compounds possess the structure of delafossite with a high symmetry of $\text{R}-3\text{m}$, and antiferromagnetically coupled magnetic ions form perfect triangular layers which are well separated along c -axis. The Curie-Weiss temperatures range from several to more than 100 kelvins. Specific heat and magnetic susceptibility down to 50 mK on NaYbO_2 , NaYbS_2 and NaYbSe_2 single crystals and polycrystals, reveal no structural or magnetic transition even at the lowest measurement temperature. The family, having the simplest structure and chemical formula among the known QSL candidates, removes the issue on disorder raised in YbMgGaO_4 . And most excitingly, the rich diversity of the family members allows tunable charge gaps, selectable exchange coupling, and many other advantages. This makes the family an ideal platform for fundamental research of QSL and its promising applications.

[†] These authors contributed to the work equally.

[‡] qmzhang@iphy.ac.cn

Introduction

The concept of quantum spin liquid was proposed by P. W. Anderson over 40 years ago^[1]. It describes a novel highly entangled spin state and was initially constructed with a superposition of spin singlets on the triangular antiferromagnet, so-called resonating-valence-bond model^[1]. Later on, the ultimate connection between QSL and high-temperature superconductivity was theoretically established through doping a QSL^[2]. The underlying topological properties in QSL were carefully studied and classified by X. G. Wen et al^[3-4]. Kitaev further demonstrated that such topological phases can be employed for the high-fidelity quantum computation^[5]. This has stimulated intensive interest in searching for QSL materials.

Quantum spin frustrated materials, particularly the spin-triangle-based antiferromagnets with strong geometrical frustration^[6], were considered to be the most likely systems realizing QSL. So far, a number of compounds have been reported to host QSL. Among them, the well-known examples include herbersmithite and its derived compounds^[7-11], and triangular organics^[12]. The magnetic ions in most of the compounds are 3d transition metal ions Cu^{2+} with $S=1/2$, which is crucial to strengthen quantum fluctuations.

On the other hand, the spin frustrated materials containing magnetic rare-earth ions are also considered to be possible QSL candidates^[13]. The spin ground state for the rare-earth ions with an odd number of f electrons (not including Gd^{3+}), is a Kramers doublet which can be mapped to a well-defined effective $S=1/2$ spin and is protected by time reversal symmetry and crystal fields^[14]. In many cases the non-Kramers rare-earth ions can also be taken as effective $S=1/2$ systems at low temperatures, though lacking the protection by time reversal symmetry^[15-16]. Therefore, rare-earth based spin-frustrated materials plays a crucial role in the exploration of QSL candidates^[13]. In fact, some QSL behaviors have been reported in several pyrochlore and spinel compounds^[17-21].

The discovery of YbMgGaO_4 has invoked increasing interest in searching for rare-earth based spin-frustrated materials^[22]. The compound has a high symmetry of $\text{R}-3\text{m}$ and Yb^{3+} ions form a flat and perfect triangular lattice^[22-23]. The availability of high-quality single crystals allows extensive and deep studies of magnetic properties using neutron scattering^[24-27], muon spin relaxation (muSR)^[28], nuclear spin resonance (NMR), electron spin resonance (ESR)^[34] etc. The studies point to the possibility of gapless QSL ground state^{[23-24][28-29]}. On the other hand, some experiments and theoretical arguments raised the

issue on Ga/Mg disorder, which was proposed to be responsible for the spin ground state and/or QSL stability^{[22],[30-32]}. The small exchange coupling ($J \sim 1$ K) allows to easily tune the spin state with a laboratory magnetic field^[22-23,29]. Meanwhile, it also requires that most experiments must be carried out at ultralow temperatures^[29,33]. In some cases this could be an obstacle for in-depth studies and possible applications.

As mentioned above, there is a long list of numerous rare-earth spin-frustrated materials^[2,13]. Then the question is if one can find out some compounds or systems with larger exchange couplings and without disorder^[6]. That is what we have done in this work. We systematically synthesized rare-earth based delafossite $AReCh_2$ (A =alkali or monovalent ions, Re =rare earth, Ch =O, S, Se) and made structural and thermodynamic characterizations. The compounds have a high symmetry of $R-3m$ and perfect spin triangular layers^[35-36]. The magnetic measurements indicate that spins are antiferromagnetically coupled in all the compounds and the Weiss temperatures vary from several to over 100 K. For the representative $NaYbCh_2$ (Ch =O, S, Se) samples, no magnetic ordering or transition is observed in the specific heat and susceptibility measurements down to 50 mK. Thus, this is a large family of QSL candidates with the simplest structure and chemical formula so far. Its crystal structure naturally removes the issue on Ga/Mg disorder proposed in $YbMgGaO_4$. The diversity of the large family makes it an ideal playground for studying QSL and exploring its promising applications.

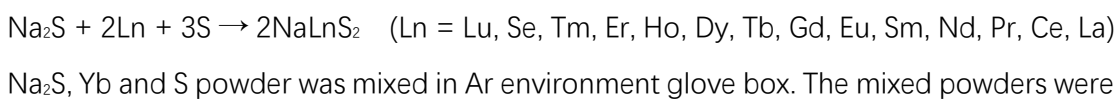
Sample preparation and experimental methods

The polycrystals of $NaLnO_2$ ($Ln = Yb, Lu$) were synthesized by the method of solid-state reaction under high temperatures:



Na_2CO_3 and Ln_2O_3 powders were mixed in a dry process (mixing molar ratio: Na_2O : Yb_2O_3 = 2.5 : 1) and shaped into a pellet by isostatic pressing (50 MPa, 2 min). Shaped samples were heated at 900°C for 9 hours. After the heating, the samples were grinded and washed with distilled water and ethanol, at last dried in air at room temperature for 48 hours.

The polycrystals of $NaLnS_2$ ($Ln=La, Ce, Pr, Nd, Sm, Eu, Gd, Tb, Dy, Ho, Er, Tm, Yb, Lu$) were synthesized by the method of solid-state reaction under high temperature:



placed in a graphite crucible and vacuum packaged with quartz tube. Packaged samples were heated at 850°C for 48 hours. After the heating, the sample were powder and washed with distilled water and then dried in air at 50 °C for 6 hours. The synthesis of polycrystals of NaLnSe_2 (Ln =Er, Yb, Lu) were similar with the synthesis of powders of NaLnS_2 . The temperature was adjusted to 900°C.

We have also successfully grown high quality NaYbSe_2 single crystals. The growth conditions of single crystals are more rigorous than NaYbSe_2 polycrystals. Na_2Se , Yb and Se powder were mixed in Ar environment glove box (mixing molar ratio: Na_2Se : Yb : Se = 1 : 2 : 12). The mixed powder was placed in special quartz tube that can withstand higher pressure. Packaged samples were headed at 1000°C for 48 hours. After the heating, we can observe 2-3 mm size single crystals.

Powder XRD profiles were measured with Bruker-D8 by step scanning. The TOPAS program was used for Rietveld crystal structure refinements. The temperature dependence of magnetic susceptibility from 1.8K to 300K was measured with a SQUID magnetometer (Quantum Design Magnetic Property Measurement System, MPMS) under both ZFC and FC for all the samples with the brass sample holder. The AC susceptibility measurements from 50mK to 4K were performed using a dilution refrigeration system (DR). The polycrystalline sample was pressed into a thin plate and fixed on a sample holder with GE vanish. The heat capacity measurements from 2K to 30K were performed using PPMS (Quantum Design Physical Property Measurement System) and DR was employed for the measurements from 50mK to 4K. The plate sample was mounted on a sample holder with N grease for better thermal contact.

Results and discussions

Fig. 1 shows the crystal structure of rare-earth delafossite and the Rietveld refinements for three representative samples NaYbO_2 , NaYbS_2 and NaYbSe_2 (Detailed structural information extracted from the refinements can be found in Supplementary Materials). Under the high symmetry of R-3m, magnetic ions form flat triangular layers which are well separated. ReCh_6 octahedra are connected by edge-sharing. The local crystal-field environment around magnetic ions is exactly analogous to the case of YbMgGaO_4 . Therefore, one may expect a crystal-field splitting of Yb^{3+} ions similar to that in YbMgGaO_4 . That means an effective $S=1/2$ spin is strictly held in this case. And similar to YbMgGaO_4 , Dzyaloshinskii-Moriya (DM) interaction is also cancelled in this case.

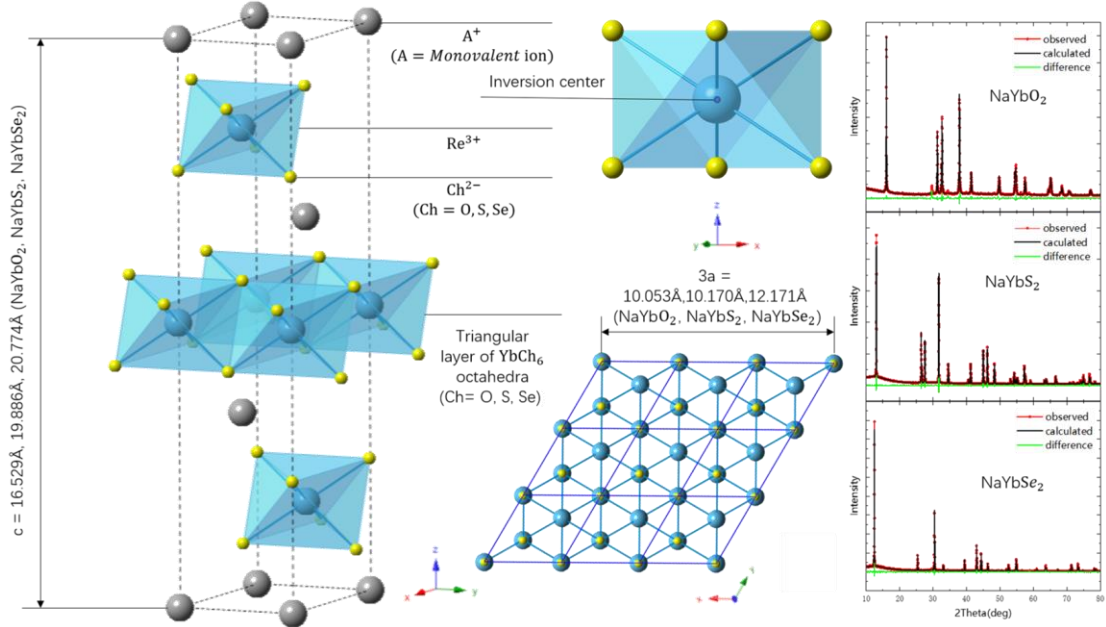


Fig. 1 General crystal structure of rare-earth chalcogenides and the powder diffraction patterns and Rietveld refinements for NaYbCh_2 ($\text{Ch}=\text{O, S, Se}$)

The Mg/Ga disorder in YbMgGaO_4 has been extensively discussed and is still under debate. In some experiments and theoretical calculations, the disorder was considered to play a dominant role in stabilizing QSL state and contributing to low-energy excitations. For comparison, there is no longer such a disorder in the family of rare-earth chalcogenides, due to the structural simplicity and high symmetry. The issue on disorder is completely removed in the family. We further made the analysis of element ratio (See Supplementary Materials), which is close to the nominal ratio. This rules out the possibility of the disorder caused by element deficiency. If one concerns about the active monovalent ions like Na^+ and K^+ , he still has plenty of choices of the heavy monovalent ones like Rb^+ , Cs^+ , Cu^+ and Ag^+ , etc.

For the selected sub-family NaYbCh_2 ($\text{Ch}=\text{O, S, Se}$), we measured DC magnetic susceptibility in the range of 2-300 K and AC susceptibility from 50mK to 4 K, which are presented in Fig. 2. The Curie-Weiss (CW) fitting was made from 150 to 300K according to the crystal-field splitting in YbMgGaO_4 and the fitting results are summarized in Table I. The negative CW temperatures suggest an antiferromagnetic coupling in all the samples. Excitingly, the CW temperatures are much larger than that of YbMgGaO_4 because of the smaller distances between nearest-neighbor Yb^{3+} in rare-earth chalcogenides. AC susceptibility for the three samples shows no sign of long-range

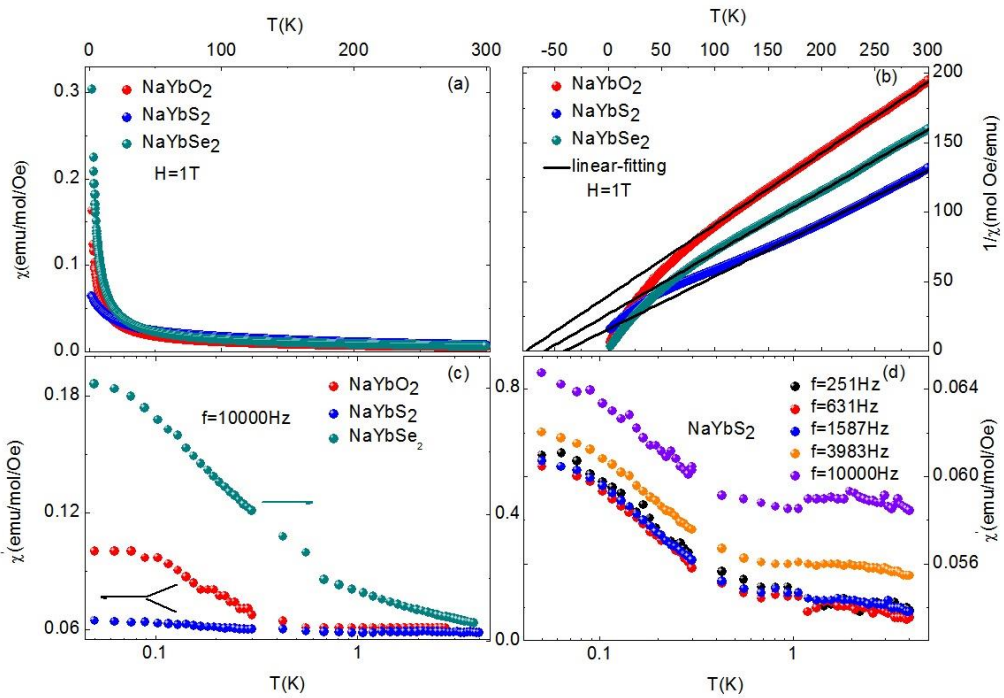


Fig. 2 DC (a & b) and AC (c & d) magnetic susceptibility of polycrystalline NaYbCh₂ (Ch=O, S, Se).

magnetic ordering. The measurements under various frequencies further confirms that there is no spin freezing either. Interestingly, the susceptibility saturation with down to zero temperature is clearly seen for all the three samples. This should be one of the consequences caused by strong spin-orbit coupling rather than a sign of finite spin excitations. The susceptibility of NaYbSe₂ at low temperatures is obviously larger than that of the other two compounds. In fact, the distance between nearest neighboring Yb³⁺ ions in NaYbSe₂ is also larger, while its CW temperatures and moment obtained from the CW fitting look comparable to the other two. The reason for this is unclear at the moment.

Table I Parameters extracted from Curie-Weiss fitting for NaYbCh₂ (Ch=O, S, Se)

Ch	Space group	C	θ_{CW} / K	μ_{eff}
O	R-3m	1.9448	-77.35	3.94
S	R-3m	2.6166	-40.98	4.57
Se	R-3m	2.2550	-59.84	4.24

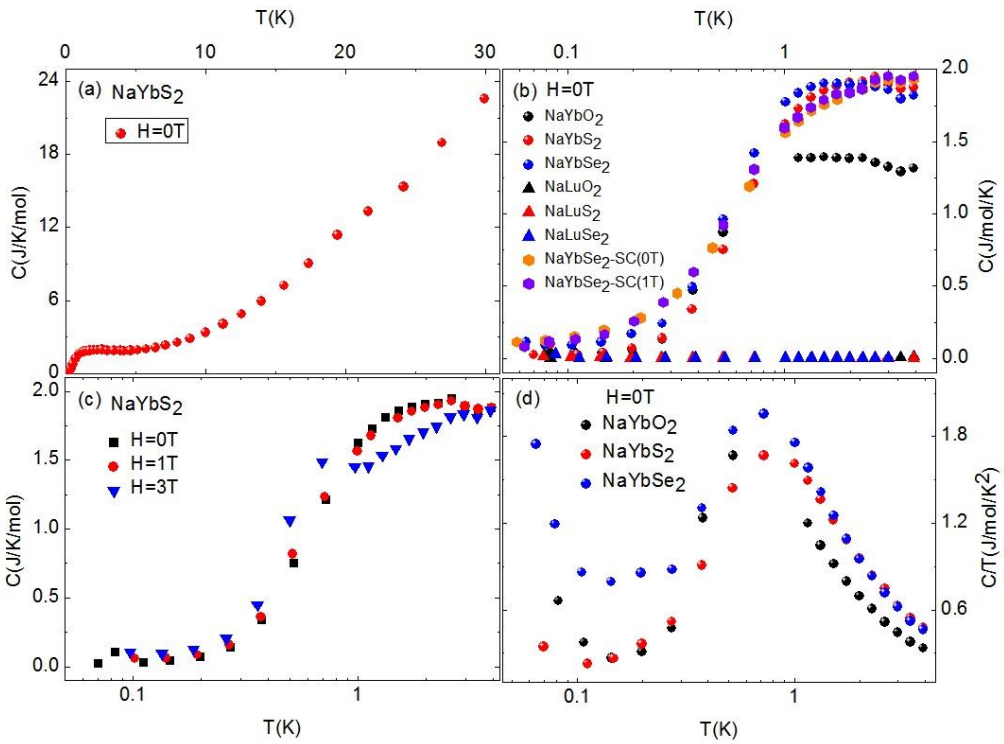


Fig. 3 Specific heat measurements on NaYbCh_2 ($\text{Ch}=\text{O, S, Se}$). Single crystal NaYbSe_2 and polycrystalline NaYbO_2 and NaYbS_2 were used in the measurements.

Specific heat results are shown in Fig. 3. There is no obvious transition down to 50 mK in the compounds, and it is consistent with the conclusion from the susceptibility experiments. We observed no apparent change or shift with applying a magnetic field up to 3 T (Fig. 3c). On the other hand, an upturn is seen below 100 mK in the $C/T \sim T$ plot (Fig. 3d). This may be contributed by nuclear spins. The upturn actually makes it hard to see the intrinsic trend of specific heat below 100 mK and to conclude that the spin ground state is gapless or gapped QSL. More magnetic and thermodynamics experiments are required in the future.

Here it should be pointed out that there is no obvious disorder in the present case and we still observed no long-range magnetic ordering or freezing which points to a possible QSL ground state. This means that the rare-earth triangular system, including rare-earth chalcogenides reported here and YbMgGaO_4 , intrinsically hosts QSL state which is not stabilized by or even originated from the Ga/Mg charge disorder.

The measurements discussed above are based on the sub-family NaYbCh_2 ($\text{Ch}=\text{O, S, Se}$). Towards a comprehensive view of the large family, we fixed Na and S, and

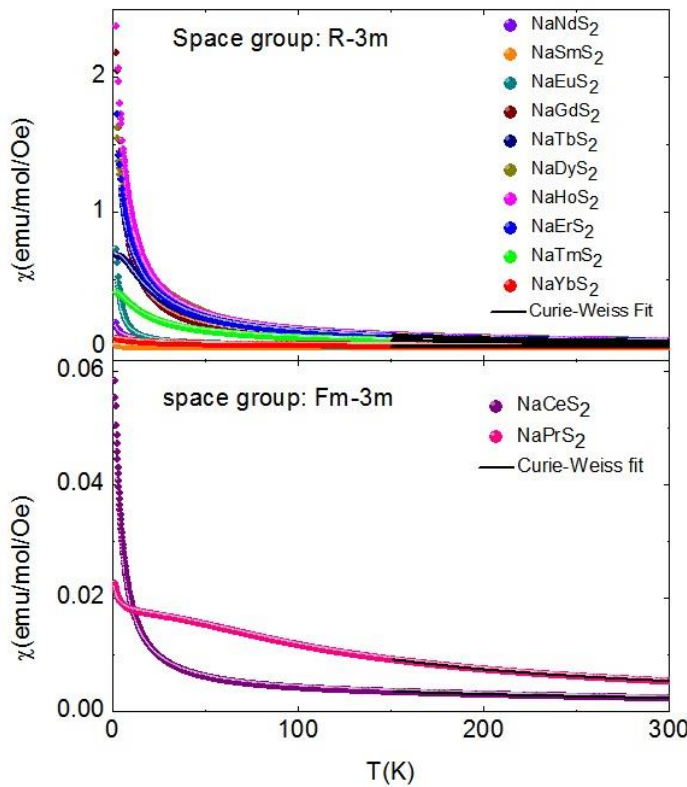


Fig. 4 Magnetic susceptibility of NaReS_2 ($\text{Re}=\text{Ce-Yb}$) in the range of 2 to 300 K.

systematically synthesized the other sub-family NaReS_2 ($\text{Re}=\text{La - Lu}$). The Rietveld refinements for all the fourteen compounds have been made and the detailed structural parameters can be found in the Supplementary Materials. The family members from Nd to Lu, keep the high-symmetry of R-3m. But the three end-members, NaLaS_2 , NaCeS_2 and NaPrS_2 show a cubic structure with the symmetry of Fm-3m. Obviously this is caused by the larger ionic radii of La, Ce and Pr. The magnetic susceptibility measurements from 2 to 300 K have been carried out on the sub-family and the results are shown in Fig. 4. No obvious magnetic transition can be seen in all the compounds with R-3m symmetry. Similar to the R-3m brothers, the cubic NaCeS_2 also shows no sign of magnetic transition from 2 to 300 K, as the perfect triangular lattice formed by magnetic ions remains undistorted and the strong geometrical frustration is always there. However, an anomaly appears around 10 K in the susceptibility of NaPrS_2 (Fm-3m).

Table II Parameters extracted from the Curie-Weiss fitting for NaReS₂ (Re=Ce-Yb)

Re	Space group	C	θ_{CW} / K	μ_{eff}	
				Obs. (μ_B)	Cal. (μ_B)
Ce	Fm-3m	1.1145	-164.42	2.99	2.54
Pr	Fm-3m	1.91757	-57.48	3.92	3.58
Nd	R-3m	1.78198	-25.35	3.77	3.62
Sm	R-3m	0.71761	-343.05	2.40	0.84
Eu	R-3m	3.19082	-106.13	5.05	3.6
Gd	R-3m	8.5521	-1.98	8.27	7.94
Tb	R-3m	12.87953	-9.49	10.15	9.72
Dy	R-3m	14.55906	-9.39	10.79	10.63
Ho	R-3m	13.8468	-5.90	10.52	10.60
Er	R-3m	12.13713	-4.62	9.85	9.59
Tm	R-3m	7.40589	-3.83	7.69	7.57
Yb	R-3m	2.90963	-63.74	4.82	4.54

The CW fitting was made from 150 to 300 K, assuming a reasonably high crystal-field splitting. The fitting results can be found in Table II. We can see that the exchange coupling changes from sample to sample. In other words, we have the opportunity to select the compounds with various exchange coupling. Beyond this, one can further tune the charge gaps of the family members by element substitution. The absorption spectra (see Supplementary Materials) indicate that the charge gaps are roughly 4.5 eV, 2.7 eV and 1.9 eV for NaYbO₂, NaYbS₂, and NaYbSe₂, respectively. These exciting advantages stem from the rich diversity of the family. In fact, we have made a careful literature research and found that most of the family members have the high-symmetry of R-3m and hence are potential QSL materials (see Supplementary Materials). This suggests that the family is an ideal playground, on which we can tune the basic material parameters or exchange coupling to explore QSL and develop its possible applications.

Summary

In this work, we synthesized rare-earth chalcogenides AReCh₂ which has a delafossite structure, and made structural and thermodynamics characterizations. The family has a high symmetry of R-3m, and magnetic ions are antiferromagnetically coupled and form

perfect triangular layers. The Curie-Weiss temperatures vary in the range of 4 K to over 100 K. Magnetic susceptibility and specific heat measurements down to 50 mK indicate no sign of long-range magnetic ordering or transition. The family removes the disorder issue raised in YbMgGaO_4 . The unique advantages, such as various charge gaps and exchange coupling, suggest that the family may be an ideal platform for the study of QSL.

Acknowledgements

We are grateful to Gang Chen for inspiring discussions. We thank Zicheng Wen for assisting absorption measurements. This work was supported by the Ministry of Science and Technology of China (2016YFA0300504 & 2017YFA0302904) and the NSF of China (11774419 & 11474357).

Author contributions

Q.M.Z proposed the original ideas and directed the whole study. W.W.L made NaLnS_2 polycrystals and grew NaYbS_2 single crystals, made structural refinement, and made specific heat and magnetic measurements and analysis. Z. Z synthesized NaYbSe_2 and NaLuSe_2 polycrystals and made refinement, and grew NaYbSe_2 single crystals. J.T.J synthesized NaYbO_2 and NaLuO_2 polycrystals and made structural characterizations. Y.X.L and H.C.L grew NaYbSe_2 single crystals. H.C.L assisted crystal growth.

References

- [1] P. Anderson, Mater. Res. Bull. 8, 153–60 (1973).
- [2] L. Savary and L. Balents, Rep. Prog. Phys. 80, 0160502 (2017).
- [3] X.G. Wen, Phys. Rev. B 40, 7387 (1989).
- [4] X.G. Wen, Phys. Rev. B 44, 2664 (1991).
- [5] A.Yu. Kitaev, Ann. Phys. 303, 2–30 (2003).
- [6] L. Balents, Nature 464, 199 (2010).
- [7] Matthew P. Shores, Emily A. Nytko, Bart M. Bartlett, and Daniel G. Nocera, J. Am. Chem. Soc. 127, 13462–3 (2005).
- [8] Philippe MENDELS and Fabrice BERT, J. Phys. Soc. Jap. 79, 011001 (2010).
- [9] Yuesheng Li, Jianlong Fu, Zhonghua Wu, Qingming Zhang, Chem. Phys. Lett. 570, 37–41 (2013).
- [10] Yuesheng Li and Qingming Zhang, J. Phys.: Condens. Matter 25, 026003 (2013).

[11] Yuesheng Li, Bingying Pan, Shiyan Li, Wei Tong, Langsheng Ling, Zhaorong Yang, Junfeng Wang, Zhongjun Chen, Zhonghua Wu and Qingming Zhang, *New J. Phys.* 16, 093011 (2014).

[12] B J Powell and Ross H McKenzie, *Rep. Prog. Phys.* 74, 056501 (2011).

[13] Jason S. Gardner, Michel J. P. Gingras, John E. Greidan, *Rev. Mod. Phys.* 82, 53 (2010).

[14] John B. Kogut, *Rev. Mod. Phys.* 51, 659 (1979).

[15] Lucile Savary and Leon Balents, *Phys. Rev. Lett.* 108, 037202 (2012).

[16] SungBin Lee, Shigeki Onoda, and Leon Balents, *Phys. Rev. B* 86, 104412 (2012).

[17] K. A. Ross, J. P. C. Ruff, C. P. Adams, J. S. Gardner, H. A. Dabkowska, Y. Qiu, J. R. D. Copley, and B. D. Gaulin, *Phys. Rev. Lett.* 103, 227202 (2009).

[18] Lucile Savary, Kate A. Ross, Bruce D. Gaulin, Jacob P. C. Ruff, and Leon Balents, *Phys. Rev. Lett.* 109, 167201 (2012).

[19] LiDong Pan, Se Kwon Kim, A. Ghosh, Christopher M. Morris, Kate A. Ross, Edwin Kermarrec, Bruce D. Gaulin, S.M. Koohpayeh, Oleg Tchernyshyov and N.P. Armitage, *Nat. Commun.* 5, 4970 (2014).

[20] LiDong Pan, N. J. Laurita, Kate A. Ross, Bruce D. Gaulin and N. P. Armitage, *Nat. Phys.* 12, 361–6 (2016).

[21] K. Kimura, S. Nakatsuji, J.-J. Wen, C. Broholm, M.B. Stone, E. Nishibori and H. Sawa, *Nat. Commun.* 4, 1934 (2013).

[22] Yuesheng Li, Haijun Liao, Zhen Zhang, Shiyan Li, Feng Jin, Langsheng Ling, Lei Zhang, Youming Zou, Li Pi, Zhaorong Yang, Junfeng Wang, Zhonghua Wu and Qingming Zhang, *Sci. Rep.* 5, 16419 (2015).

[23] Yuesheng Li, Gang Chen, Wei Tong, Li Pi, Juanjuan Liu, Zhaorong Yang, Xiaoqun Wang, and Qingming Zhang, *Phys. Rev. Lett.* 115, 167203 (2015).

[24] Yuesheng Li, Devashibhai Adroja, David Voneshen, Robert I. Bewley, Qingming Zhang, Alexander A. Tsirlin and Philipp Gegenwart, *Nat. Commun.* 8, 15814 (2016).

[25] Yuesheng Li, Devashibhai Adroja, Robert I. Bewley, David Voneshen, Alexander A. Tsirlin, Philipp Gegenwart and Qingming Zhang, *Phys. Rev. Lett.* 118, 107202 (2017).

[26] Xinshu Zhang, Fahad Mahmood, Marcus Daum, Zhiling Dun, Joseph A. M. Paddison, Nicholas J. Laurita, Tao Hong, Haidong Zhou, N. P. Armitage and Martin Mourigal, *Phys. Rev. X* 8, 031001 (2018).

[27] Yao Shen, Yao-Dong Li, Hongliang Wo1, Yuesheng Li, Shoudong Shen, Bingying Pan, Qisi Wang, H. C. Walker, P. Steffens, M. Boehm, Yiqing Hao, D. L. Quintero-Castro, L. W.

Harriger, M. D. Frontzek, Lijie Hao, Siqin Meng, Qingming Zhang, Gang Chen and Jun Zhao, *Nature* 540, 20614 (2016).

[28] Yuesheng Li, Devashibhai Adroja, Pabitra K. Biswas, Peter J. Baker, Qian Zhang, Juanjuan Liu, Alexander A. Tsirlin, Philipp Gegenwart, and Qingming Zhang, *Phys. Rev. Lett.* 117, 097201 (2016).

[29] Y. Xu, J. Zhang, Y. S. Li, Y. J. Yu, X. C. Hong, Q. M. Zhang, and S. Y. Li, *Phys. Rev. Lett.* 117, 267202 (2016).

[30] Yao-Dong Li, Yao Shen, Yuesheng Li, Jun Zhao, and Gang Chen, *Phys. Rev. B* 97, 125105 (2018).

[31] F. Alex Cevallos, Karoline Stolze, Robert J. Cava, *Solid State Commun.* 276, 5–8 (2018).

[32] Zhenyue Zhu, P. A. Maksimov, Steven R. White, and A. L. Chernyshev, *Phys. Rev. Lett.* 119, 157201 (2017).

[33] Itamar Kimchi, Adam Nahum, and T. Senthil, *Phys. Rev. X* 8, 031028 (2018).

[34] Zhu-Xi Luo, Ethan Lake, Jia-Wei Mei and Oleg A. Starykh1, *Phys. Rev. Lett.* 120, 037204 (2018).

[35] Bin Deng, Donald E. Ellis, and James A. Ibers, *Inorganic Chem.* 41, 22 (2002).

[36] A. K. Gray, B. R. Martin and P. K. Dorhout, *New Crystal Struct.* 218, 1.19 (2003).

Supplementary Materials

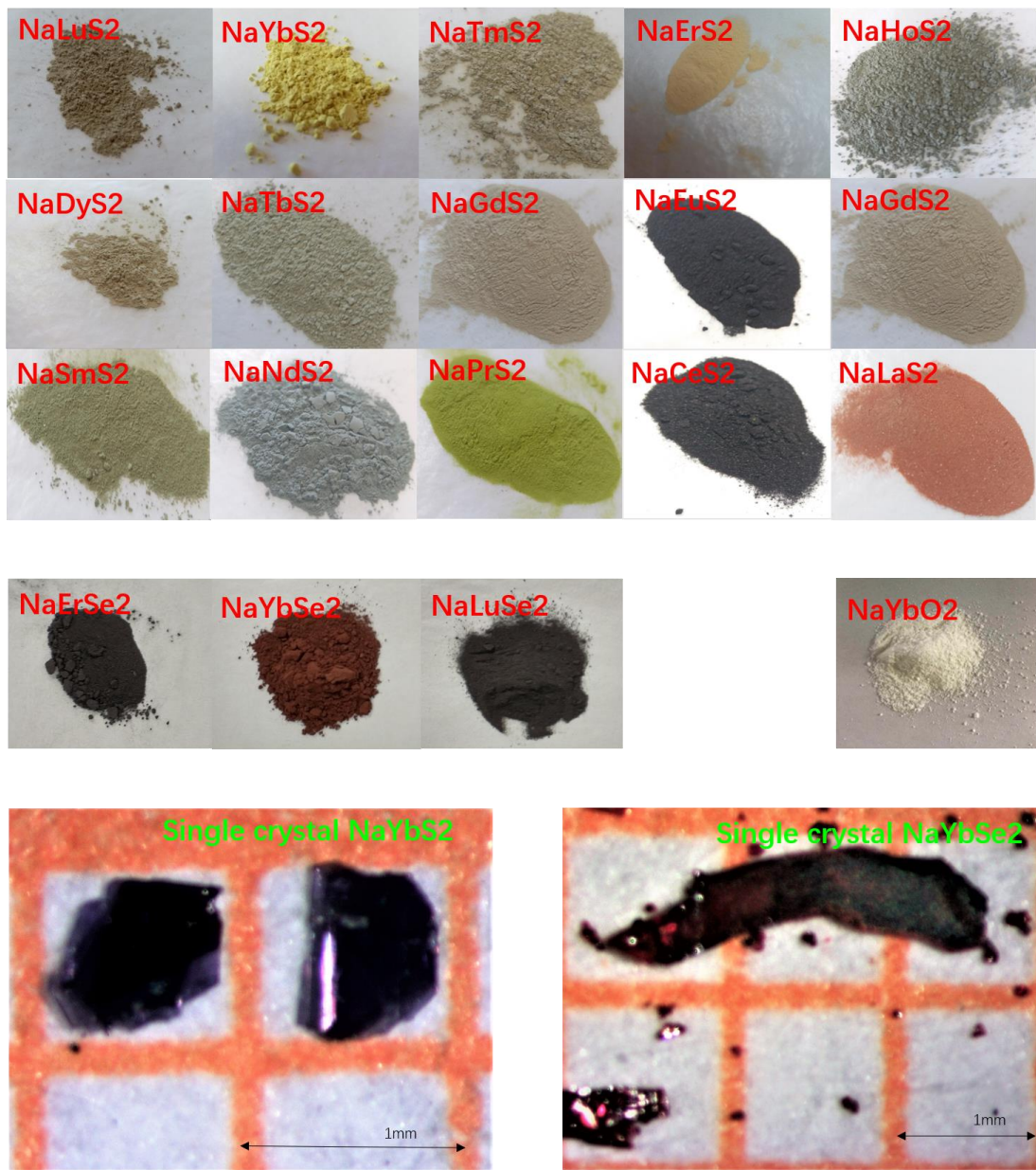


Fig. S1 Photos of NaReCh₂ polycrystals and single crystals (Ch=O, S, Se; Re=La-Lu).

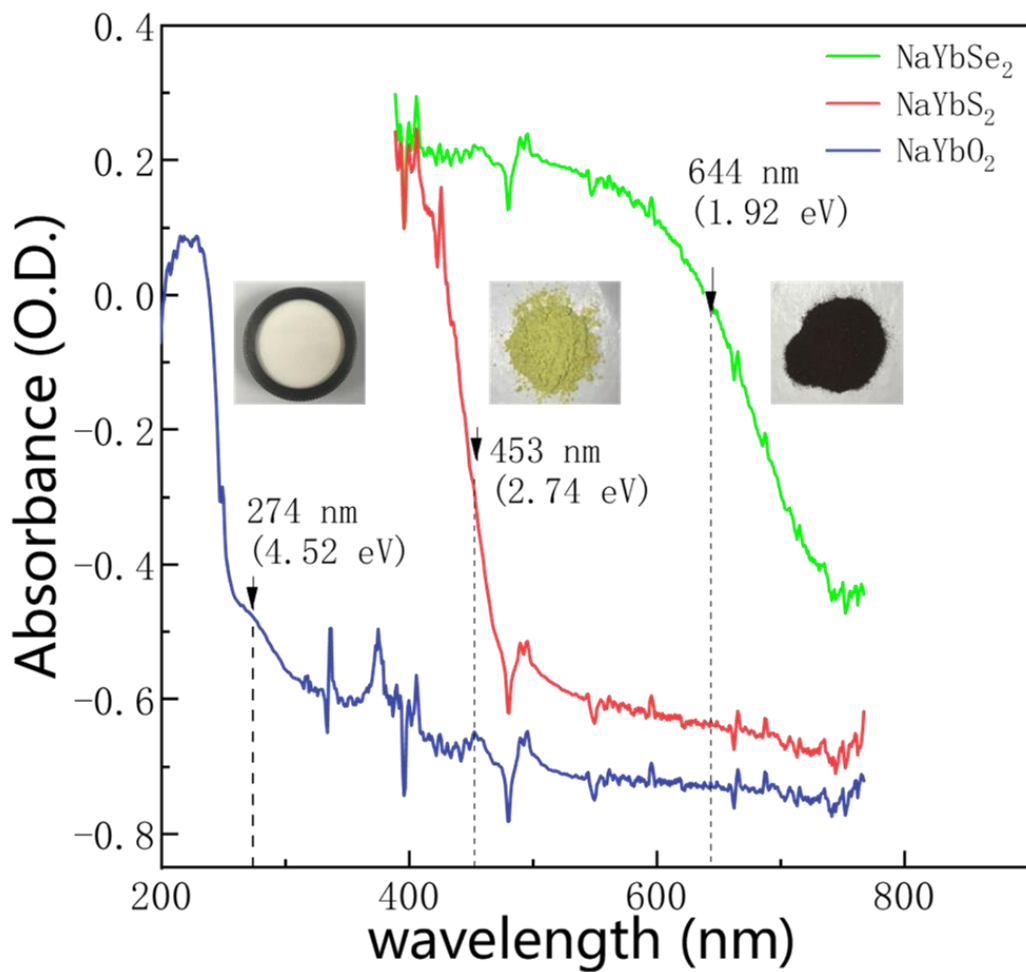


Fig. S2 Absorption spectra of NaYbCh_2 polycrystals ($\text{Ch}=\text{O, S, Se}$).

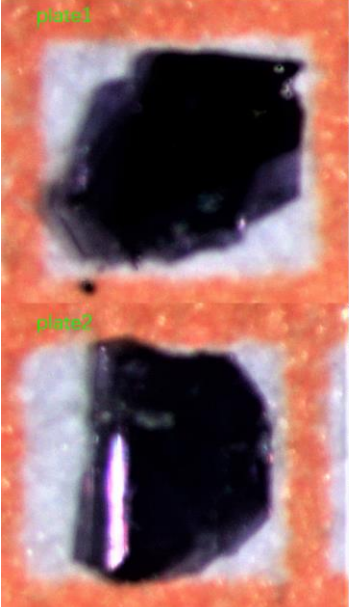


plate1	Atom percent					
	1	2	3	4	5	average
Na	24.26	24.50	25.20	24.33	25.62	24.782
Yb	24.18	24.15	22.94	24.11	22.08	23.492
S	51.56	51.34	51.86	51.56	52.30	51.724
Total	100	100	100	100	100	99.998
Na:Yb:S	1.06:1:2.2					
plate2	Atom percent					
	1	2	3	4	5	average
Na	24.20	24.37	22.77	23.95	24.51	23.96
Yb	24.68	24.24	23.73	23.93	24.41	24.198
S	51.13	51.38	53.50	49.94	51.07	51.404
Total	100	100	100	100	100	99.562
Na:Yb:S	0.99:1:2.12					

Fig. S3 Element ratio analyzed by EDX method

Table S1 Powder diffraction and structural parameters given by Rietveld refinement.

X-ray diffraction and structural refinement for NaYbCh2 (Ch=O, S, Se)				
Compounds		NaYbO ₂	NaYbS ₂	NaYbSe ₂
Radiation		Cu K_{α}	Cu K_{α}	Cu K_{α}
Temperature		300K	300K	300K
Symmetry		R-3m	R-3m	R-3m
Lattice constants	a = b	3.35113Å	3.90839Å	4.05753Å
	c	16.5292Å	19.88553Å	20.7744Å
Cell volume	V	160.7547Å ³	263.06573Å ³	296.1973Å ³
Crystal size	L	443.3nm	800nm	1409.8nm
	G	137.6nm	200nm	3612.0nm
Residuals	Rwp	0.07509	0.04754	0.08207
Atom sites				
Na ⁺	x = y	0	0	0
	z	0.5	0.5	0.5
Occupancy		1	1	1
Yb ³⁺	x = y	0	0	0
	z	0	0	0
Occupancy		1	1	1
Ch ²⁻ (Ch = O, S, Se)	x = y	0	0	0
	z	0.25744	0.25835	0.25811
Occupancy		1	1	1
Selected interatomic distance				
Yb-Ch(Ch = O, S, Se)		3.148Å	3.249Å	3.283Å
Yb-Yb		3.35113Å	3.90839Å	4.05753Å
Distance between adjacent Yb ³⁺ layers	d = c/3	5.41973Å	6.62851Å	6.82480Å

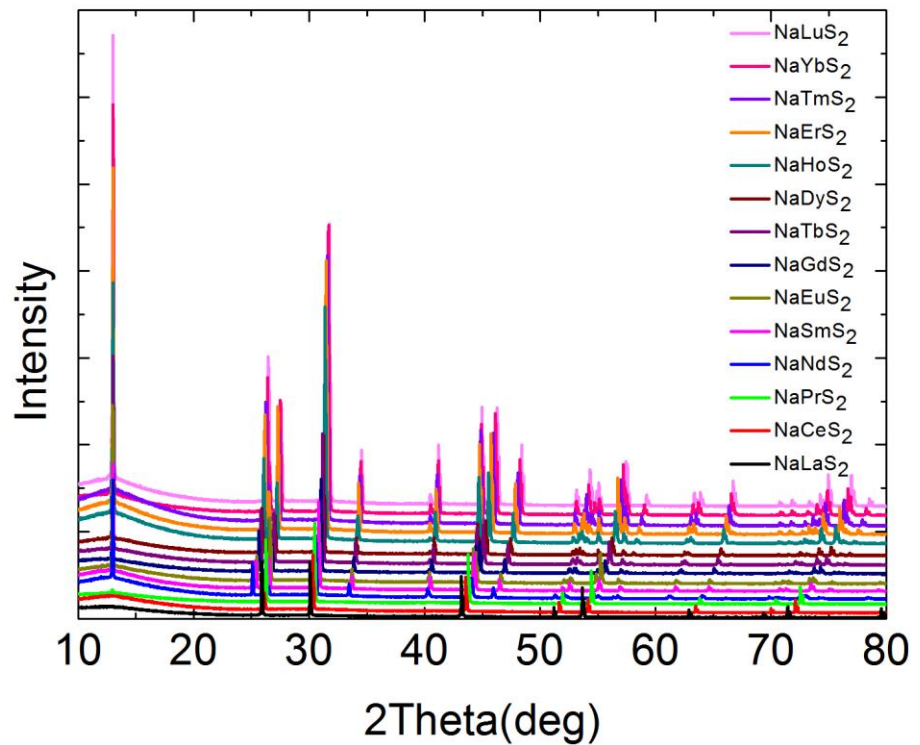


Fig. S4 X-ray diffraction patterns for NaReS_2 ($\text{Re}=\text{La-Lu}$).

Table S2 Structural parameters of NaReS₂ (Re=La-Lu) extracted from Rietveld refinement.

	Space group	$a\left(\text{\AA}^0\right)$	$c\left(\text{\AA}^0\right)$	$V\left(\text{\AA}^0\text{ }^3\right)$	$R_{wp}\left(\%\right)$
<i>NaLaS</i> ₂	<i>Fm\overline{3}m</i>	5.88564		203.88318	10.361
<i>NaCeS</i> ₂	<i>Fm\overline{3}m</i>	5.83911		199.08539	3.958
<i>NaPrS</i> ₂	<i>Fm\overline{3}m</i>	5.80706		195.82505	7.631
<i>NaNdS</i> ₂	<i>R\overline{3}m</i>	4.10792	19.93425	291.32228	3.873
<i>NaSmS</i> ₂	<i>R\overline{3}m</i>	4.06054	19.91429	284.35656	3.976
<i>NaEuS</i> ₂	<i>R\overline{3}m</i>	4.05160	19.99367	284.23395	5.699
<i>NaGdS</i> ₂	<i>R\overline{3}m</i>	4.02044	19.93933	279.11896	4.079
<i>NaTbS</i> ₂	<i>R\overline{3}m</i>	3.99581	19.91911	275.42901	4.934
<i>NaDyS</i> ₂	<i>R\overline{3}m</i>	3.97570	19.91535	272.61305	3.936
<i>NaHoS</i> ₂	<i>R\overline{3}m</i>	3.95743	19.91548	270.11410	3.733
<i>NaErS</i> ₂	<i>R\overline{3}m</i>	3.94007	19.90959	267.67098	3.926
<i>NaTmS</i> ₂	<i>R\overline{3}m</i>	3.92351	19.89094	265.17629	3.468
<i>NaYbS</i> ₂	<i>R\overline{3}m</i>	3.90839	19.88553	263.42901	4.754
<i>NaLuS</i> ₂	<i>R\overline{3}m</i>	3.89552	19.89603	261.47335	4.793

Table S3 Basic parameters of the existing AReO₂ (A=monovalent ions, Re=Rare earth). T_{min}, θ_{CW} and μ_{eff} are the lowest measurement temperature, Curie-Weiss temperature and effective spin moment, respectively.

	O	La	Ce	Pr	Nd	Sm	Eu	Gd	Tb	Dy	Ho	Er	Tm	Yb	Lu	Y	
Space group		P2 ₁ /c	pbnm	pbnm	P2 ₁ /c	P2 ₁ /c	P2 ₁ /c	P2 ₁ /c	I4 ₁ /amd	I4 ₁ /amd	I4 ₁ /amd	I4 ₁ /amd					
T _{min} / K	Li	1.8	1.8	1.8	1.8	1.8	1.8	1.8	1.8	1.8	1.8	1.8	1.8	1.8	1.8	1.8	
θ _{CW} / K																	
μ _{eff}				3.56	3.44	1.49	3.35	7.68	9.63	10.03	10.30	9.38	7.45	4.65			
Space group		I4 ₁ /amd	C2/c	C2/c	C2/c	C2/c	C2/c	R̄3m	R̄3m	R̄3m	R̄3m						
T _{min} / K					1.8	1.8	1.8			1.8	1.8	1.8	1.8	1.8			
θ _{CW} / K	Na				2.53			-		-	-	-	-	-			
μ _{eff}						3.49	1.59	3.25	7.59		10	10.0	8.75	7.14	4.48		
Space group		R̄3m		R̄3m	R̄3m	R̄3m	R̄3m	R̄3m	R̄3m	R̄3m	R̄3m	R̄3m	R̄3m	R̄3m	R̄3m	R̄3m	
T _{min} / K	K				1.8	1.8	1.8	1.8	1.8	1.8	1.8	1.8	1.8	1.8	1.8	1.8	
θ _{CW} / K					-80			-11.3	-29.1	-18.6	-608	-12.8	-18.8	-77			

μ_{eff}					3.79	1.57	3.49	7.75	9.23	10.33	10.09	9.35	7.00	4.31		
Space group	Rb	$R\bar{3}m$			$R\bar{3}m$	$R\bar{3}m$	$R\bar{3}m$	$R\bar{3}m$		$R\bar{3}m$	$R\bar{3}m$	$R\bar{3}m$	$R\bar{3}m$	$R\bar{3}m$		
T_{min} / K																
θ_{CW} / K																
μ_{eff}																
Space group	Cs				<i>P63/mmc</i>											
T_{min} / K																
θ_{CW} / K																
μ_{eff}																
Space group	Ag												$R\bar{3}m$	$R\bar{3}m$	$R\bar{3}m$	
T_{min} / K													1.8	1.8	1.8	
θ_{CW} / K													-34	-66		
μ_{eff}													7.52	4.46		

Table S4 Basic parameters of the existing AReS₂ (A=monovalent ions, Re=Rare earth). T_{min}, θ_{CW} and μ_{eff} are the lowest measurement temperature, Curie-Weiss temperature and effective spin moment, respectively.

Table S5 Basic parameters of the existing AReSe₂ (A=monovalent ions, Re=Rare earth). T_{min}, θ_{CW} and μ_{eff} are the lowest measurement temperature, Curie-Weiss temperature and effective spin moment, respectively.

	Se	La	Ce	Pr	Nd	Sm	Eu	Gd	Tb	Dy	Ho	Er	Tm	Yb	Lu	Y
Space group	Li				<i>Fm</i> 3 <i>m</i>	<i>Fm</i> 3 <i>m</i>		<i>R</i> 3 <i>m</i>	<i>R</i> 3 <i>m</i>	<i>R</i> 3 <i>m</i>	<i>R</i> 3 <i>m</i>				<i>R</i> 3 <i>m</i>	
T _{min} / K					77	77		77	77	77	77	77				
θ _{CW} / K					-20.3			4	-12	7.6	-6.7	-9.1				
μ _{eff}					3.54	1.08		7.67	9.78	10.15	10.54	9.39				
Space group	Na	<i>R</i> 3 <i>m</i>	<i>R</i> 3 <i>m</i>		<i>R</i> 3 <i>m</i>	<i>R</i> 3 <i>m</i>		<i>R</i> 3 <i>m</i>	<i>R</i> 3 <i>m</i>	<i>R</i> 3 <i>m</i>	<i>R</i> 3 <i>m</i>		<i>R</i> 3 <i>m</i>		<i>R</i> 3 <i>m</i>	
T _{min} / K			77		77			77	77	77	77	77				
θ _{CW} / K			-73.7		-4.4			5.6	-2	-10.7	-1.2	4.1				
μ _{eff}			2.3		3.34	1.16		7.61	10.27	10.88	10.54	9.05				
Space group	K					<i>R</i> 3 <i>m</i>								<i>R</i> 3 <i>m</i>		
T _{min} / K																
θ _{CW} / K																
μ _{eff}																
Space group	Rb	<i>R</i> 3 <i>m</i>	<i>R</i> 3 <i>m</i>	<i>R</i> 3 <i>m</i>	<i>R</i> 3 <i>m</i>	<i>R</i> 3 <i>m</i>	<i>R</i> 3 <i>m</i>	<i>R</i> 3 <i>m</i>	<i>R</i> 3 <i>m</i>	<i>R</i> 3 <i>m</i>	<i>R</i> 3 <i>m</i>	<i>R</i> 3 <i>m</i>	<i>R</i> 3 <i>m</i>	<i>R</i> 3 <i>m</i>	<i>R</i> 3 <i>m</i>	
T _{min} / K			5							5			5			
θ _{CW} / K			-113.1							-2.58			-4.8			

